International Journal of Pharmaceutics 422 (2012) 238–244

Contents lists available at SciVerse ScienceDirect

International Journal of Pharmaceutics

journal homepage: www.elsevier.com/locate/ijpharm

Surface energy analysis as a tool to probe the surface energy characteristics of micronized materials—A comparison with inverse gas chromatography

John F. Gamble[a,*], Michael Leane[a], Dolapo Olusanmi[a], Michael Tobyn[a], Enes Šupuk[b], Jiyi Khoo[c], Majid Naderi[c]

[a] Drug Product Science & Technology/Materials Science, Bristol-Myers Squibb, Reeds Lane, Moreton, Wirral, CH46 1QW, UK
[b] Institute of Particle Science and Engineering, University of Leeds, Leeds, LS2 9JT, UK
[c] Surface Measurement Systems Ltd., Alperton, Middlesex, HA0 4PE, UK

ARTICLE INFO

Article history:
Received 29 July 2011
Received in revised form 6 October 2011
Accepted 3 November 2011
Available online 10 November 2011

Keywords:
Physical properties
Inverse gas chromatography
Surface energy
Micronization
Pharmaceuticals

ABSTRACT

This study investigates the impact of micronization on the measured surface energy characteristics of an active pharmaceutical ingredient (API), *Ibipinabant*, by inverse gas chromatography (IGC) using both a fixed probe concentration, commonly used in standard IGC methods, and a fixed probe surface coverage approach applied by the surface energy analyzer (SEA), a next generation IGC system.

The IGC measurements indicate an initial increase in surface energy, going from un-micronized to micronized, followed by a reduction in surface energy with increasing micronization extent. This was attributable to the change in the retention behaviour of the dispersive probes as a consequence of the change in the probe surface coverage rather than a change in the actual surface energy of the materials being analysed.

It was observed in the SEA data that micronization leads to an increase in the measured dispersive surface energy of the drug substance with increasing micronization extent. The increase in surface energy is primarily due to the generation of new, higher energy interaction sites, although a small additional increase is also observed which is related to the increase in the number and distribution of high energy sites.

The results demonstrate that in order to obtain comparable surface energetic data between batches with varied surface area, and presumably between different materials, results should be obtained at a specific, and constant, probe surface coverage.

1. Introduction

Micronization is a commonly used technique within the pharmaceutical industry often used to produce particles in the 1–30 μm range. Air jet micronization is a process that uses high pressure air to micronize friable materials into ultra-fine powders. The high pressure expanding air jets are used to entrain and accelerate the particles within the mill chamber. The induced high speed rotation subjects the entrained materials to undergo high speed particle–particle collisions which create increasingly smaller particles. Screens are used to classify the maximum particle size limit, with particle too large to pass through the screen remaining within the chamber for further milling. The impact of this aggressive milling process on particle properties is an area of significant interest within the pharmaceutical industry.

Over the course of the last 30 years, inverse gas chromatography (IGC) has become an established tool for the investigation of the surface energy characteristics of non-volatile materials within the pharmaceutical industry. With the introduction of the new surface energy analyzer (SEA) the probe injection approach has been altered. Instead of using the fixed partial pressure injection method traditionally utilized by standard IGC systems, the SEA applies, with knowledge of the sample surface area, a range of targeted surface coverages, which can then be used to regress back to the 0% coverage dispersive surface energy for a sample. This latter approach should provide truly comparable results between samples, removing any ambiguity relating to differences in probe coverage due to differences in particle characteristics such as surface area. This clarification in surface coverage may enable better correlation of the measured surface energy parameters of materials with other surface characteristics. Inverse gas chromatography is a powerful technique capable of determining the surface energy components of an 'unknown' sample, acting as the stationary phase, which is packed into a silanised glass column. The surface energy components are determined from the retention times of a range of 'known'

* Corresponding author. Tel.: +44 0151 552 1646; fax: +44 0151 552 1650.
E-mail address: john.gamble@bms.com (J.F. Gamble).

0378-5173/$ – see front matter © 2011 Elsevier B.V. All rights reserved.
doi:10.1016/j.ijpharm.2011.11.002

dispersive and polar probes (the mobile phase) which interact with the surface of the sample (Thielmann, 2004). The net retention volume (V_N), a fundamental surface thermodynamic property of the solid–vapour interaction, is obtained from Eq. (1):

$$V_N = \frac{j}{m} \cdot F \cdot (t_R - t_0) \cdot \left(\frac{T}{273.15}\right) \quad (1)$$

where j is the James–Martin correction, m is the mass of sample in the column (g), F is the carrier gas flow rate (cm^3/min), t_R is the retention time of the probe (minutes), t_0 is the mobile phase hold-up time (minutes), and T is the column temperature in Kelvin (K). Surface energy can be described as the sum of the dispersive and specific contributions. Dispersive (apolar) interactions, also known as Lifshitz–van der Waals interactions, consist of London interactions which originate from electron density changes (the force between two instantaneously induced dipoles) but may also include both Keesom (the force between two permanent dipoles) and Debye (the force between a permanent dipole and a corresponding induced dipole) interactions. Specific (polar) interactions explain all other types of interactions. The dispersive component (γ_S^D) can be calculated from the retention time of a series of n-alkane probes injected at infinite dilution (probe concentrations within the Henry's portion of the sorption isotherm, where the change of probe–probe interaction is assumed negligible and any retention is therefore only due to probe–solid interactions), typically using the relationship (Eq. (2)) proposed by Schultz et al. (1987):

$$RT \ln V_N = a \cdot (\gamma_L^D)^{1/2} \cdot 2N_A \cdot (\gamma_S^D)^{1/2} + C \quad (2)$$

where R is the universal gas constant (J/mol K), a is the molecular cross sectional area of adsorbates (m^2), N_A is Avogadro's number, γ_L^D is the dispersive component of surface free energy of the liquid probe (J/m^2), γ_S^D is the dispersive component of the free energy of the solid (J/m^2), and C is a constant.

The dispersive component of the free energy is thus obtained from the gradient of a plot of $RT \ln V_N$ versus $a(\gamma_L^D)^{1/2}$. The specific contributions for the polar probes are obtained from the specific free energy of adsorption (ΔG) which is the vertical distance of the polar probe from the dispersive probe reference plot. Using the Gutmann (1978) approach liquids can be described in terms of their electron accepting and electron donating properties, and are accordingly assigned an acceptor (AN*) and/or donor (DN) number. If the entropic contributions are assumed to be negligible (Papirer et al., 1988), the acid–base interactions of polar probes with a solid surface can be described using Eq. (3):

$$-\Delta G = K_A \cdot DN + K_D \cdot AN^* \quad (3)$$

The Lewis acid (K_A) and base (K_D) parameters for a range of polar probes can therefore be obtained from the slope and intercept respectively of a plot of ($-\Delta G/AN^*$) versus DN/AN^* in accordance with Eq. (4):

$$\frac{-\Delta G}{AN^*} = \left(\frac{DN}{AN^*}\right) K_A + K_D \quad (4)$$

The van Oss (1994) concept divides the specific component of surface energy into an acid (Lewis acceptor), γ_s^+, and a base (Lewis donor), γ_s^- contribution, the values of which can be obtained from the specific free energy using Eq. (5):

$$-\Delta G = N_A \cdot a \cdot 2 \cdot ((\gamma_L^+ \times \gamma_S^-)^{1/2} + (\gamma_L^- \times \gamma_S^+)^{1/2}) \quad (5)$$

If monopolar acidic and basic probes (such as chloroform and ethyl acetate) are used the specific component of the surface energy can be determined using just two probes by means of an abbreviated version of the Owens and Wendt (1969) approach (Eq. (6)):

$$\gamma_S^{SP} = 2\sqrt{(\gamma^- \times \gamma^+)} \quad (6)$$

An alternative to the Schultz approach for determining the dispersive component (Eq. (7)) was proposed by Dorris and Gray (1980):

$$\gamma_S^D = \frac{[RT \ln(V_{N(C_{n+1}H_{2n+4})})/V_{N(C_nH_{2n+2})}]}{4N_A^2 \cdot a_{CH_2}^2 \cdot \gamma_{CH_2}} \quad (7)$$

where a_{CH_2} is the surface area of a CH_2 unit (~6 Å^2) and γ_{CH_2} is its free energy (approximately 35.6 mJ/m^2). Although the value for γ_{CH_2} was based originally on a vapour–liquid interaction, a similar value for solid-vapour interactions is likely as Dorris and Gray showed that, for the adsorption process from an ideal gas phase to an ideal adsorbed phase, the adsorbability is independent of the chain length of a homologous series of the alkanes. With respect to the use of the cross-sectional area of a CH_2 group, Dorris and Gray assumed the area occupied by a CH_2 group in the surface is the same as the cross-sectional area that it occupies in a parallel arrangement of n-alkane chains in the bulk liquid. Previously, Aveyard et al. (1972) indicated that the reorientation of the chains may contribute little to the work of adhesion and also indicated that the alkanes have the same parallel orientation at the liquid–liquid and the vapour–liquid interfaces. As an overall consequence, the Dorris and Gray approach has been shown to have less dependence on the probe input parameters, than the Schultz method (Shi et al., 2011). When the Dorris and Gray approach is used the dispersive component of the surface energy is obtained from a plot of $RT \ln V_N$ versus the carbon number of the alkane solutes. For this approach the specific free energy of absorption values are obtained from a plot of $RT \ln V_N$ versus the molar deformation polarization (Dong et al., 1989) of the probes, P_D, which is obtained using Eq. (8):

$$P_D = \frac{(MW \cdot (r^2 - 1))}{(\rho_l \cdot (r^2 + 2))} \quad (8)$$

where MW is the molar mass of the probe, r is the reflective index of the probe, and ρ_l is the probe liquid density.

Both approaches for the determination of the dispersive component have been demonstrated to yield comparable results (Voekel et al., 2008). One basic assumption of the both approaches is that the retention behaviour of the dispersive probes is independent of the injection size, and this assumption has only recently been started to be probed with work to determine the impact of probe volume (surface coverage) on the measured retention volume (Ho et al., 2010, 2011; Ylä-Mäihäniemi et al., 2008).

Applications of IGC are wide ranging and include the monitoring of batch-to-batch variation (Gamble et al., 2010; Ticehurst et al., 1996), the impact of different processing routes (Thielmann et al., 2007), the detection of low levels of process induced disorder (Feeley et al., 1998), investigating the interactions of excipients and drug substances (Tay et al., 2010; Traini et al., 2008), and the relationship of polar data with tribo-electric charging of materials (Ahfat et al., 2000) to name but a few.

The use of IGC for monitoring the impact of milling processes, such as micronization, on the surface properties of materials has been another of the more widely reported applications (Balard et al., 2008; Chamarthy and Pinal, 2008; Heng et al., 2006; York et al., 1998). The finding of these studies commonly indicate that the milling process leads to an increase in the dispersive surface energy of a material with the increase in surface energy often being attributed to the relative exposure of newly created, higher energy crystal faces and/or amorphous sites due to particle fracture/breakage. However, a number of researchers have also reported a reduction in dispersive surface energy with milling (Ohta and Buckton, 2004; Otte and Carvajal, 2010), an observation which has been suggested to result from annealing of the surface.

One factor often overlooked in these investigations, however, is the impact of the change in surface area achieved through a

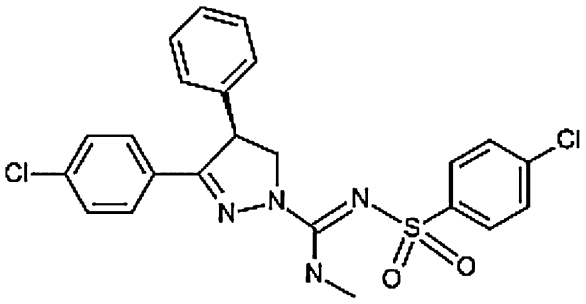

Fig. 1. Structure of *Ibipinabant*.

milling process on the retention behaviour of the dispersive probes. Although the technique itself is particle size/surface area independent as a consequence of the use of an infinite probe injection volume, this does not necessarily mean that a change in the surface area cannot itself impact the measured dispersive surface energy. One could argue that a significant change in the surface area of a sample is indeed equivalent to a change in the probe injection size as the surface coverage of a probe, and hence the distribution of energetic sites interacted with, may change when injected at a constant probe volume. An additional complication is that such differences in sample surface areas may also affect each of the probes to varying degrees; the vapour pressure of each probe will determine the actual number of probe molecules injected and so probes with relatively fewer probe molecules may be more affected by a change in sample surface area compared to those with higher numbers of probe molecules. Hence a situation could be proposed where a change in the measured surface energy could be achieved through an alteration of the width of the distribution of energetic sites/probe interactions, i.e. a change in probe surface coverage as a consequence of a shift in surface area, rather than a change in the surface energy *per se*. In all likelihood, any change in dispersive surface energy is likely be a mixture of mechanisms, but to elucidate the impact of milling it is important to separate increases in energy due to the generation of higher energetic sites (e.g. through crystalline disruption and/or exposure of new higher energy crystal faces) from any possible energy increase due to the change in surface area. With the introduction of the new SEA this distinction can now be more readily investigated. The aim of this study was to investigate the impact of micronization on the surface energy characteristics of an active pharmaceutical ingredient (API), *Ibipinabant*, using both fixed probe concentration (IGC) and fixed probe surface coverage (SEA) approaches.

2. Materials

The material (Fig. 1) used during this study was *Ibipinabant*, a poorly soluble (Biopharmaceutical Classification System class II) drug substance, which had been micronized using a MC-200 jetmill (Jetpharma, Balerna, Switzerland) to varying levels; additionally an un-micronized batch of the drug was also analysed during the study. The micronization conditions are detailed in Table 1, with the milling energy ($\bar{E}$) defines in Eq. (9):

$$\bar{E} = \frac{P \times F}{M} \tag{9}$$

where P is the milling pressure (kN/m^2), F is the feed rate (kg/min), and M is the mass of material milled (kg).

Table 1
Micronization process conditions.

Batch reference	Pressure (bar)	Feed rate (g/min)	Milling energy (kN m^{-2} min^{-1})
7B30504	N/A	N/A	N/A
7C31536	1.5	120	150
7C31538	12	4	200
7C31560	2	100	300
7C31562	3	80	1200

3. Methods

3.1. Inverse gas chromatography

The dispersive surface energy of samples was determined by inverse gas chromatography using both a SMS–IGC and a SEA–IGC (both from Surface Measurement Systems, Alperton, Middlesex, UK). The samples were packed into 0.3 m (3 mm inside diameter) silanised glass columns, plugged at either end by silanised glass wool. The samples were conditioned at 30 °C (303 K), 0% RH, 10 cm^3/min for 2 h prior to analysis. The same sample columns were tested in both systems so as to remove any sample packing differences. The methods used for each system are detailed below.

3.1.1. SEA

A range of dispersive probes; undecane, decane, nonane, octane, heptane, and hexane were injected at a range of fractional surface coverages (0.15–20%) in order to determine the concentration free dispersive surface energy (i.e. the dispersive surface energy at 0% probe coverage). The polar free energy of adsorption analysis was determined using a range of polar probes; 1,4-dioxane, acetone, acetonitrile, chloroform, ethyl acetate, and ethanol at an equivalent range of fractional surface coverages as used for the dispersive probes. The column dead time was determined using an inert probe, methane (0.208 cm^3 injection volume). For the purposes of comparison, the values reported are nominally the 5% surface coverage values as well as the regressed 0% coverage results. The dispersive component was obtained using the Dorris and Gray approach and the polar components obtained using the polarization approach. Due to the long analysis times for the SEA heterogeneity method, samples were not analysed in replicate. The variability between measurements for the SEA instrument is notably lower than IGC as the system uses the same pipe line and injection manifold for every injection, thus the standard deviation of the measurement is small, typically ~2%, and much smaller for low surface energy materials.

3.1.2. IGC

A range of dispersive probes; decane, nonane, octane, heptane, and hexane were injected at a partial pressure of $0.03p/p_0$. Two polar probes; ethyl acetate and chloroform were also injected at the same partial pressure as used for the dispersive probes. The column dead time was determined using an inert probe (methane at $0.2p/p_0$). The dispersive component was obtained using the Schultz approach. The same columns were used for both SEA and IGC methods. The micronized samples were analysed in triplicate, and the un-micronized sample was analysed in duplicate.

3.2. Specific surface area

The samples were analysed using a Gemini 2390A surface area analyser (Micromeritics, Norcross, USA). Samples were out-gassed for 70 h at 50 °C under nitrogen gas prior to analysis. Samples were then evacuated at a rate of 500 mmHg/min for 5 min and equilibrated for 5 min. Multipoint measurements (8 points) over the range of $0.05–0.3p_0$ were performed, and linearity within the B.E.T. range confirmed.

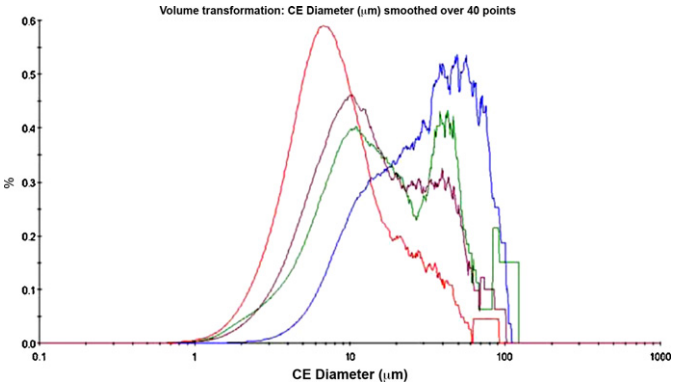

Fig. 2. Geometric (volume based) particle size distributions of micronized batches (red = 7C31538; maroon = 7C31562; green = 7C31560; blue = 7C31536).

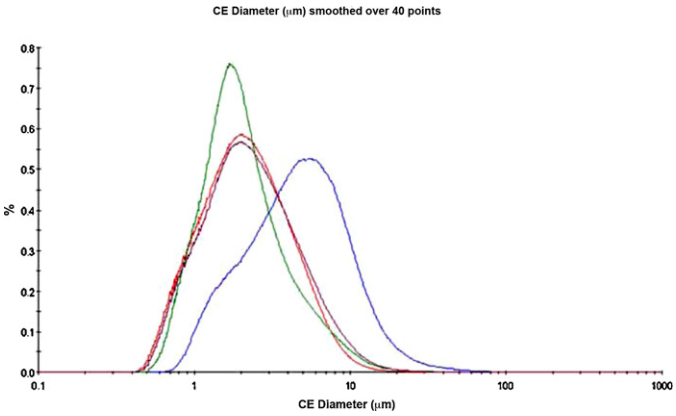

Fig. 3. Arithmetic (number based) particle size distributions of micronized batches (red = 7C31538; maroon = 7C31562; green = 7C31560; blue = 7C31536).

3.3. Particle size

The particle size of the materials was determined using a Morphologi G3S particle characterisation system (Malvern Instruments Limited, Malvern, UK). Samples were wet dispersed in iso-octane (containing less than 0.1% lecithin) and then pipette onto microscope slides prior to analysis. Particle imaging was conducted using a 20× magnification lens (1.8–100 μm resolution range) with *z*-stacking enabled (taking 3 additional planes above the point of focus, equivalent to 16.3 μm) to account for some degree of three-dimensionality within the sample. Morphological filtering was applied on a sample by sample basis in order to remove any aggregated and/or overlapping particles from the final analysis (Gamble et al., 2011).

3.4. Scanning electron microscopy (SEM)

The samples were sputter coated using a JFC-1300 auto fine coater (Jeol Inc, MA, USA) and then imaged using a Neoscope JCM-500 (Jeol Inc., MA, USA).

4. Results and discussion

4.1. Surface energy analyzer results

The dispersive surface energy results from the SEA (at a surface coverage of 5%) are shown in Table 2. The 5% coverage value was selected as it incorporated most of the range of higher energetic sites available in the analysed samples. The results demonstrate an inversely proportional relationship with the median geometric particle size whilst the surface area is observed to be directly proportional. Comparison of the geometric (volume based) and arithmetic (number based) particle size data (Figs. 2 and 3, respectively) indicates a bimodal geometric distribution and a skewed normal arithmetic distribution. This suggests that the geometric median size is closely linked to the presence of a relatively small population of partially micronized (large volume, low surface area) particles, an observation that is corroborated by SEM analysis (Fig. 4). This would also suggest that the energetic sites for interaction of these larger particles must therefore be notably lower in energy than that of the micronized material, as the available surface for interaction for these large volume (and also low population density) particles is significantly smaller than for the micronized particles, and this is indeed observed for the un-micronized sample.

The regressed to 0% coverage dispersive surface energy values for three of the four micronized samples are observed to follow a similar pattern as the 5% coverage results (an explanation for the deviation for the forth sample will be dealt with subsequently); the data indicates that the dispersive surface energy at both 0% and 5% coverage increases with the extent of micronization, with the change in the 5% data seen to be slightly more pronounced than that of the 0% data.

The surface energy heterogeneity data (Fig. 5), a map of dispersive surface energies over a range of probe surface coverages, shows that as the materials are further micronized there is an increase in the energy of the highest energy sites (0% coverage) available for interaction, and hence a shift in the position of the distribution. The heterogeneity distribution for the un-micronized material is observed to indicate a wide range of energetic sites available, but the shape of the distribution would suggest that the high energy sites are noticeably lower in number (indicated by a much steeper decline with surface probe coverage) than the micronized batches.

However, the heterogeneity data for the micronized batches also suggests that as the surface area increases, the range of energetic sites that the dispersive probes interact with narrows, such that the obtained mean dispersive surface energy could be expected to further increase, due to probes interacting primarily with a narrow range of higher energy sites due to the increase in surface area/number of sites available for interaction, as previously

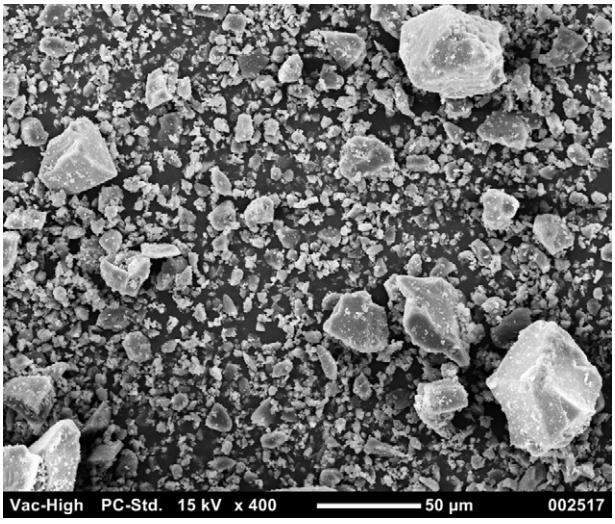

Fig. 4. SEM image for batch #7C31536.

Table 2
Summary of results.

Batch reference	Geometric particle size, D_{50} (μm)	Specific surface area (m^2/g)	Dispersive surface energy (mJ/m^2)			ΔG_{SEA} at 5% coverage (kJ/mol)		ΔG_{IGC} at $0.03p/p_0$ (kJ/mol) (SD)	
			SEA (at 0% coverage)	SEA (at 5% coverage)	IGC (at $0.03p/p_0$) (SD)	Ethyl acetate	Chloroform	Ethyl acetate	Chloroform
7B30504	79.10	0.20	47.77	32.29	40.56 (0.45)	5.74	5.19	6.87 (0.01)	0.31 (0.01)
7C31536	32.08	1.08	41.45	35.43	50.78 (0.38)	6.22	5.70	7.67 (0.06)	0.52 (0.02)
7C31560	16.47	1.53	48.17	39.71	47.12 (0.08)	6.20	5.61	8.08 (0.01)	0.56 (0.05)
7C31562	13.08	1.42	44.70	40.19	49.84 (0.64)	6.14	5.58	8.05 (0.03)	0.91 (0.08)
7C31538	7.785	4.32	45.44	42.30	46.38 (0.33)	5.45	4.96	8.63 (0.06)	0.79 (0.04)

suggested. The subtle difference in the slope between the dispersive surface energy at both 0% and 5% coverage would therefore suggest that the increase in the dispersive surface energy is primarily related to the generation of new, higher energetic probe interaction sites and/or exposure of crystal faces with higher energy than the habit faces (indicated by the 0% results). However, an additional increase in the measured surface energy (at 5% surface coverage) with increasing micronization extent is also observed due to a narrowing of the probe interaction distribution as a consequence of an increase in the relative number of high energy faces available for interaction.

As previously noted one of the batches, 7C31560, does not follow the previously discussed trends (e.g. dispersive surface energy versus specific surface area) as well as may be expected, but rather appears to have a similar energy distribution to the un-micronized material. The surface area data for this batch is also observed to be slightly lower than expected for the measured particle size which indicates that the width of the particle size distribution has changed. This batch is clearly observed to have a notably higher than expected '0% coverage' energy, but also a wider distribution of energetic interactions thus drawing the mean dispersive surface energy value obtained by both systems down although the impact on the IGC data is more significant due to the additional decrease in probe surface coverage. This would suggest that although a material of target particle size has been achieved during micronization, the surface energy characteristics are not aligned with the other batches as the sample has a higher than expected energy at low surface coverages combined with a wider distribution (lower number) of median energy sites) than would have been predicted from the other three micronized samples.

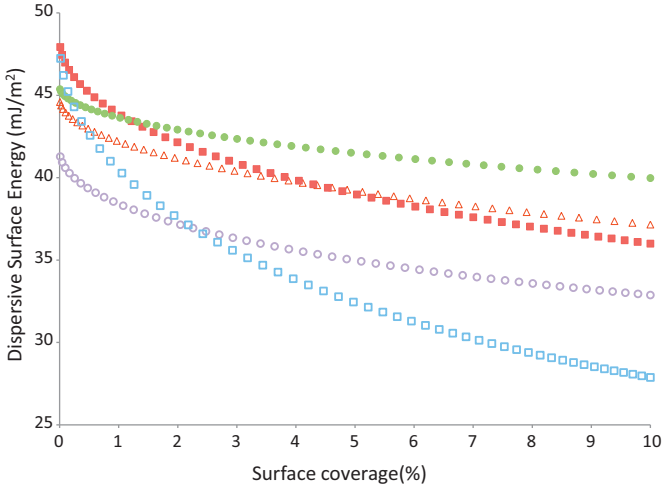

Fig. 5. Surface heterogeneity results at between 0% and 10% surface probe coverage for batches having undergone varying mill energies. 7C31562 (1200 kN m^{-2} min^{-1}) [Δ] 7C31560 (300 kN m^{-2} min^{-1}) [■], 7C31538(200 kN m^{-2} min^{-1}) [▲], 7C31536(150 kN m^{-2} min^{-1}) [○] and 7B30504 (un-micronized) [□].

4.2. Comparison of IGC and SEA data

To investigate the impact of the probe injection method on the measured dispersive surface energy results, the samples were also tested on a traditional IGC instrument using a fixed volume probe injection approach. In theory, due to the use of a fixed volume injection approach, the IGC (at a partial pressure of $0.03p/p_0$) would be more susceptible to the impact of the change in surface area, and so one could argue that as surface area increases the agreement between IGC and SEA results should reduce due to IGC results overestimating the actual increase. The results do indeed demonstrate a divergence between IGC and SEA, however, interestingly the results for the micronized samples are inverse of the expected trend with the agreement between the results increasing with increasing surface area. The results also show an inverse relationship to each other, with the IGC data suggesting, after an initial increase from the un-micronized material, a decrease in the dispersive surface energy of the material with micronization extent/surface area. As previously discussed, the mechanism which has been proposed by other authors for such a reduction in the dispersive surface energy of a material with increasing extent of milling has been suggested to be due to annealing of the surface prior to analysis. However, with the SEA data showing an inverse relationship to the IGC data this mechanism cannot be attributed as both sets of data were generated on the same sample columns. In this circumstance the reason for the difference must be related to the difference in the probe volume approaches used by the two systems.

As the IGC method uses a fixed volume, based on partial pressure, the actual number of probe molecules injected will differ for each probe in line with their respective vapour pressure, hence an equivalent volume injection of a higher carbon number dispersive probe will introduce less probe molecules than a lower carbon number probe at an equivalent partial pressure and temperature. When the probe surface coverage for each of the dispersive probe injections in the IGC method are calculated, the results (Fig. 6) demonstrate that the retention volumes of the higher carbon number dispersive probes are affected to a greater degree by the change in the sample surface area; for example hexane retention volume is 6.6 ml/g at a surface area of 1.1 m^2/g and reduces to 2.1 ml/g at a surface area of 4.3 m^2/g (31.8% reduction), compared to 819 ml/g and 217 ml/g (73.5% reduction) respectively for decane. This would indicate that an increase in the retention time of all probes would be observed with increasing sample surface area; however, the increase would become more pronounced with increasing dispersive probe carbon chain length. As a consequence, the value for the gradient of the plot of net retention volume ($RT\ln V_N$) versus the vapour surface property $(a(\gamma_{LV}^{d})^{0.5})$ is observed to decrease with increasing surface area, thereby artificially decreasing the resultant measured dispersive surface energy. The equivalent plots for the SEA data shows that the gradient is observed to increase with surface area. This would explain the observed inverse relationship in the dispersive surface energy values obtained from the two systems, and would also suggest that the actual change in surface

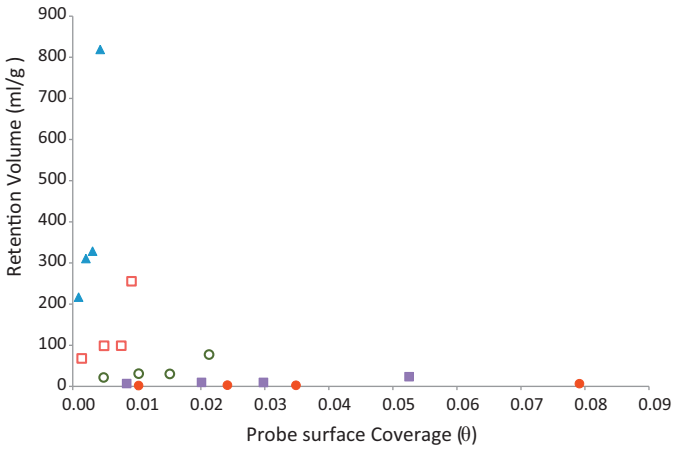

Fig. 6. Effect of surface area on the IGC dispersive probe retention volume: decane (▲), nonane (□), octane (○), heptane (■), and hexane (●).

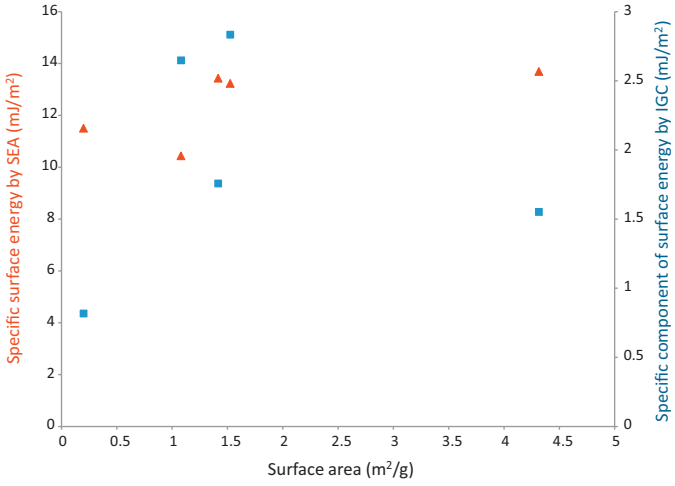

Fig. 7. Plot of specific component of surface energy versus surface area for IGC (●) and SEA (■) analyses.

energy is generally small such that its impact in the IGC data is over-shadowed by the effect of the surface area on the probe surface coverage.

The same types of trend are also observed in the polar probe data which leads to significantly greater variability in the calculated specific component of the surface energy values from the IGC when compared to those obtained from the SEA (Fig. 7). The data from the SEA shows a gradual increase in the specific component of the surface energy of the material with increasing surface area (and milling extent), whilst the IGC data does not indicate any clear relationship. The source of this error could reside in the observation that the free energy of absorption values for chloroform show an order of magnitude difference between the two systems. This variability in the free energy of adsorption results, and hence any derived Lewis acid–base numbers (K_A and K_D), obtained using IGC data will have a direct impact on any analyses where the polar probe data is to be used to correlate to another material characteristic, for example, Ahfat et al. (2000) who found a 'possible' relationship between a ratio of the Lewis acid–base numbers of a range of materials with their propensity for tribo-electric charging.

5. Conclusions

A comparison of the dispersive surface energy data for the materials analysed using fixed probe volume (IGC) and fixed surface coverage (SEA) methods enabled comparison of the results obtained from both systems. The results indicated that the fixed probe volume (IGC) data was inherently more sensitive to changes in the physical properties of the material being analysed, and as a consequence reported a reduction in surface energy with increasing surface area. This apparent reduction in the dispersive surface energy measured by IGC with increasing milling energy was shown to be partly attributable to the change in the retention behaviour of the dispersive probes, as a consequence of the change in the probe surface coverage. The change in probe surface coverage in the IGC data was demonstrated to affect a change in the measured surface energy due to the probe injection volume remaining constant whilst the sample surface area varied. The impact of the change in surface area was also demonstrated to have a variable effect on each of the dispersive probes, with the lower carbon number dispersive probes observed to be significantly more sensitive to the change in the sample surface area, thus explaining the observed decrease in dispersive surface energy with surface area for the IGC data. Equivalent probe variability was also observed for the polar probe data.

The results, as measured by SEA, demonstrated that micronization did lead to an increase in the measured dispersive surface energy and surface area, of the drug substance with an increasing extent of micronization. Through use of the SEA data at varied surface coverages the measured increase was found to be primarily related to the generation of new higher energy interaction sites. A small additional increase related to the increase in the number of high energy sites, and thus a narrowing of the energy distribution, was also demonstrated.

It is clear from these results that in order to obtain comparable surface energetic data between batches with varied surface area, and presumably between different materials, results should be obtained at a specific, and constant, probe surface coverage.

Acknowledgements

The authors would like to thank Dr. Philip Attwool (Surface Measurement Systems), Prof. Mojtaba Ghadiri (University of Leeds), Dr. Nancy Barbour, Dr. John Grosso, and Dr. Peter Timmins (all Bristol-Myers Squibb) for their support during this study.

References

Ahfat, N.M., Buckton, G., Burrows, R., Ticehurst, M.D., 2000. An exploration of interrelationships between contact angle, inverse phase gas chromatography and triboelectric charging data. Eur. J. Pharm. Sci. 9, 271–276.
Aveyard, R., Briscoe, B.J., Chapman, J., 1972. J. Chem. Soc. Faraday Trans. 1 68, 2255.
Balard, H., Maafa, D., Santini, A., Donnet, J.B., 2008. Study by inverse gas chromatography of the surface properties of milled graphites. J. Chromatogr. A 1198–1199, 173–180.
Chamarthy, S.P., Pinal, R., 2008. The nature of crystal disorder in milled pharmaceutical materials. Colloids Surf. A: Phys. Eng. Aspects 331, 68–75.
Dong, S., Brendlé, M., Donnet, J.B., 1989. Study of solid surface polarity by inverse gas chromatography at infinite dilution. Chromatographia 28, 469–472.
Dorris, G.M., Gray, D.G., 1980. Adsorption of *n*-alkanes at zero surface coverage on cellulose paper and wood fibres. J. Colloid Interface Sci. 77, 353–362.
Feeley, J.C., York, P., Sumby, B.S., Dicks, H., 1998. Determination of surface properties and flow characteristics of salbutamol sulphate, before and after micronisation. Int. J. Pharm. 172, 89–96.
Gamble, J.F., Chiu, W.-S., Gray, V., Toale, H., Tobyn, M., Wu, Y., 2010. Investigation into the degree of variability in the solid state properties of common pharmaceutical excipients – anhydrous lactose. AAPS PharmSciTech 11, 1552–1557.
Gamble, J.F., Chiu, W.-S., Tobyn, M., 2011. Investigation into the impact of subpopulations of agglomerates on the particle size distribution and flow properties of conventional microcrystalline cellulose grades. Pharm. Dev. Technol. 16, 542–548.
Gutmann, V. (Ed.), 1978. The Donor–Acceptor Approach to Molecular Interactions. Plenum Press, New York, pp. 17–33.
Heng, J.Y.Y., Thielmann, F., Williams, D.R., 2006. The effects of milling on the surface properties of form I paracetamol crystals. Pharm. Res. 23, 1918–1927.
Ho, R., Muresan, A.S., Hebbink, G.A., Heng, J.Y.Y., 2010. Influence of fines on the surface energy heterogeneity of lactose for pulmonary drug delivery. Int. J. Pharm. 388, 88–94.

Ho, R., Dilworth, S.E., Williams, D.R., Heng, J.Y.Y., 2011. Role of surface chemistry and energetics in high shear wet granulation. Ind. Eng. Chem. Res. 50, 9642–9649.
Ohta, M., Buckton, G., 2004. Determination of the changes in surface energetic of cefditoren pivoxil as a consequence of processing induced disorder and equilibration to different relative humidities. Int. J. Pharm. 269, 81–88.
Otte, A., Carvajal, M.T., 2010. Assessment of milling-induced disorder of two pharmaceutical compounds. J. Pharm. Sci., doi:10.1002/jps.22415.
Owens, D.K., Wendt, R.C., 1969. J. Appl. Polym. Sci. 13, 1741.
Papirer, E., Balard, H., Vidal, A., 1988. Inverse gas chromatography: a valuable method for the surface characterisation of fillers for polymers (glass fibres and silicas). Eur. Polym. J. 24, 783–790.
van Oss, C.J., 1994. Interfacial Forces in Aqueous Media. Marcel Dekker, New York.
Schultz, L., Lavielle, C., Martin, J., 1987. The role of the interface in carbon fibre-epoxy composites. J. Adhes. 23, 45–60.
Shi, B., Wang, Y., Jia, L., 2011. Comparison of Dorris–Gray and Shultz methods for the calculation of surface dispersive free energy by inverse gas chromatography. J. Chromatogr. A. 1218, 860–862.
Tay, T., Das, S., Stewart, P., 2010. Magnesium stearate increases salbutamol sulphate dispersion: what is the mechanism? Int. J. Pharm. 383, 62–69.
Thielmann, F., 2004. Introduction into the characterisation of porous materials. J. Chromatogr. A 1037, 115–120.
Thielmann, F., Burnett, D.J., Heng, J.Y.Y., 2007. Determination of the surface energy distributions of different processed lactose. Drug Dev. Ind. Pharm. 33, 1240–1253.
Ticehurst, M.D., York, P., Rowe, R.C., Dwivedi, S.K., 1996. Characterisation of the surface properties of α-lactose monohydrate with inverse gas chromatography, used to detect batch variation. Int. J. Pharm. 141, 93–99.
Traini, D., Young, P.M., Thielmann, F., Acharya, M., 2008. The influence of lactose pseudopolymorphic form on salbutamol sulfate–lactose interactions in DPI formulations. Drug Dev. Ind. Pharm. 34, 992–1001.
Voekel, A., Batko, K., Adamska, K., Strzemiecka, B., 2008. Determination of Hansen solubility parameters by means of gas–solid inverse gas chromatography. Adsorp. Sci. Technol. 26, 93–102.
Ylä-Mäihäniemi, P.P., Heng, J.Y.Y., Theilmann, F., Williams, D.R., 2008. Inverse gas chromatographic method for measuring the dispersive surface energy distribution for particulates. Langmuir 24, 9551–9557.
York, P., Ticehurst, M.D., Osborn, J.C., Roberts, R.J., Rowe, R.C., 1998. Characterisation of the surface energetics of milled dl-propanol hydrochloride using inverse gas chromatography and molecular modelling. Int. J. Pharm. 74, 179–186.